Elastic and inelastic scattering of 1.5-MeV neutrons by the even-A isotopes of zirconium and molybdenum*

F. D. McDaniel,† J. D. Brandenberger, G. P. Glasgow, and H. G. Leighton‡
Department of Physics and Astronomy, University of Kentucky, Lexington, Kentucky 40506
(Received 31 January 1974)

Differential elastic and inelastic cross sections were measured for 1.5-MeV neutrons scattered by the even-A isotopes of zirconium and molybdenum. The scattering samples were enriched isotopes of ^{90}Zr, ^{92}Zr, ^{94}Zr, ^{92}Mo, ^{94}Mo, ^{96}Mo, and ^{100}Mo. The cross sections were measured using a dynamically biased neutron time-of-flight spectrometer. The differential cross sections have root-mean-square relative and normalization uncertainties of 2 to 3.5% and 7 to 7.5%, respectively, for elastic scattering, and 6 to 13% and 9 to 15%, respectively, for inelastic scattering. Isotopes with similar level structures have almost identical elastic angular distributions. The entire set of data was theoretically fitted using the optical-statistical model with resonance-width-fluctuation corrections. The calculated elastic differential cross section was assumed to be an incoherent sum of shape-elastic and compound-elastic scattering. At the minima in the angular distributions the cross sections were dominated by compound-elastic scattering.

[NUCLEAR REACTIONS ^{90,92,94}Zr, ^{92,94,96,100}Mo(n, n), (n, n'), E_n=1.5 MeV; measured $\sigma(\theta)$; deduced optical model parameters. Isotopically enriched samples, neutron time of flight, dynamic bias, compound-elastic scattering, level width fluctuations.]

I. INTRODUCTION

An extensive study of neutron elastic and inelastic scattering in the mass $A=90$ region is in progress at this laboratory.[1-12] Data have been taken over a period of several years to study neutron scattering and scattering mechanisms in the incident neutron energy range of 1.5 to 8.6 MeV. The study encompasses five even-A isotopes of Mo and three even-A isotopes of Zr, Mo with $A=92$ to 100 and Zr with $A=90$ to 94. The entire set of cross sections, both elastic and inelastic, is now in the process of being analyzed with a consistent set of optical model parameters. This paper reports the study of elastic and inelastic scattering of 1.5 MeV neutrons by seven nuclei in the mass region $A=90$ to 100: ^{90}Zr, ^{92}Zr, ^{94}Zr, ^{92}Mo, ^{94}Mo, ^{96}Mo, ^{100}Mo. A lower limit of 1.5 MeV was chosen for the study because Lambropoulos *et al.*[13] have made an extensive set of cross section measurements for the Mo isotopes and for natural molybdenum from 0.1 to 1.5 MeV.[13,14]

II. EXPERIMENTAL APPARATUS

The neutron differential cross sections were measured using a dynamically biased neutron time-of-flight (TOF) spectrometer.[15-17] The dynamically biased neutron TOF spectrometer was developed at the University of Kentucky as a means for reducing the high backgrounds typically associated with neutron scattering experiments.

The University of Kentucky Model CN Van de Graaff accelerator was used to produce monoenergetic neutrons using the $T(p, n)^3$He reaction. For the TOF experiments the accelerator beam was terminally pulsed at 2.0 MHz and had a pulse width of less than 10 nsec. The beam pulse width was further shortened to less than 1.0 nsec by a Mobley beam pulse compression system.[18-20] The beam, collimated by a 0.48 cm aperture, was passed through a 0.000 36 cm Mo foil into a tritium gas cell. The cylindrical gas cell was made of thin walled stainless steel 0.8 cm in diameter and 3.0 cm in length and was lined with tantalum 0.025 cm thick. The tritium gas pressure was maintained at a pressure of 1.0 atm. The proton energy loss in passing through the Mo foil and the 3.0 cm of ^{3}H gas was 231 keV and 83 keV, respectively. The neutron energy produced at 0° at the center of the gas cell was 1.5 MeV. The total spread in neutron energy was 84 keV.

The experimental arrangement is shown in Fig. 1. The massive detector shield, mounted on a goniometer, is used to reduce the room-scattered background, the neutrons striking the detector directly from the source, and other accelerator associated backgrounds. Two neutron detectors were used in these measurements since the experiments for Mo and Zr were done at different times because of the limited availability of the isotopically enriched samples. Both detectors were NE 218 liquid organic scintillators, 10.0 cm in

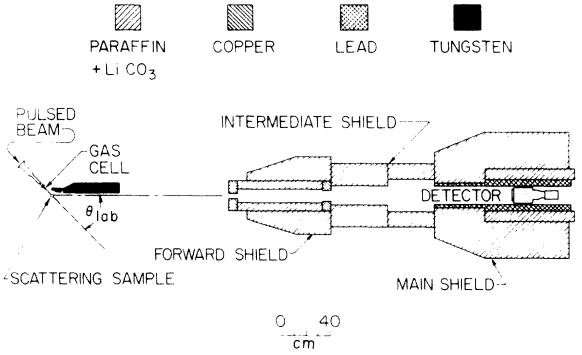

FIG. 1. Experimental apparatus consisting of the tritium gas cell, scattering sample, detector, and shield.

diameter. The scintillator used for the Mo measurements was 1.3 cm thick and the scintillator used for the Zr measurements was 5.0 cm thick. Each scintillator was mounted on an RCA bi-alkali phototube. The shielded detector could be rotated from $-100°$ to $+160°$ with respect to the accelerator beam axis.

The dynamic biasing technique was used in these neutron scattering experiments. This technique was developed in this laboratory and is described in detail elsewhere.[17] The essential feature of this technique is that the TOF of a neutron is used by an on-line computer to set both an upper and lower bias level on the pulse height from the detector for that particular detection event. The results are a background reduction in the time spectra of a factor of 4, and the ability to work with a large dynamic range for neutron detection. The schematic diagram for this system is shown in Fig. 2. Figure 3 shows the computer logic flow for the dynamic biasing. The conventional TOF spectrum is accumulated simultaneously in a multichannel analyzer for visual monitoring during the data run.

A conventional TOF spectrum was also obtained for the monitor detector, which was mounted 1.0 m above the tritium gas target. This monitor was in a polyethylene shield and collimator, and viewed the neutron source directly. The output signals from its time to amplitude converter (TAC) were sent to a single channel analyzer, and a window was placed around the TOF peak of direct monoenergetic neutrons from the gas target. This almost entirely eliminated uncorrelated background and prompt γ rays. The scaled outputs of the single channel analyzer were used to normalize the neutron flux for each data run.

III. DIFFERENTIAL CROSS SECTION MEASUREMENTS

The cylindrically shaped scattering samples were enriched isotopes of molybdenum and zirconium and are described in Table I. Cross sections were measured for only four of the even-A Mo isotopes because the ^{98}Mo sample was not available at the time of the Mo experiment. Also included in Table

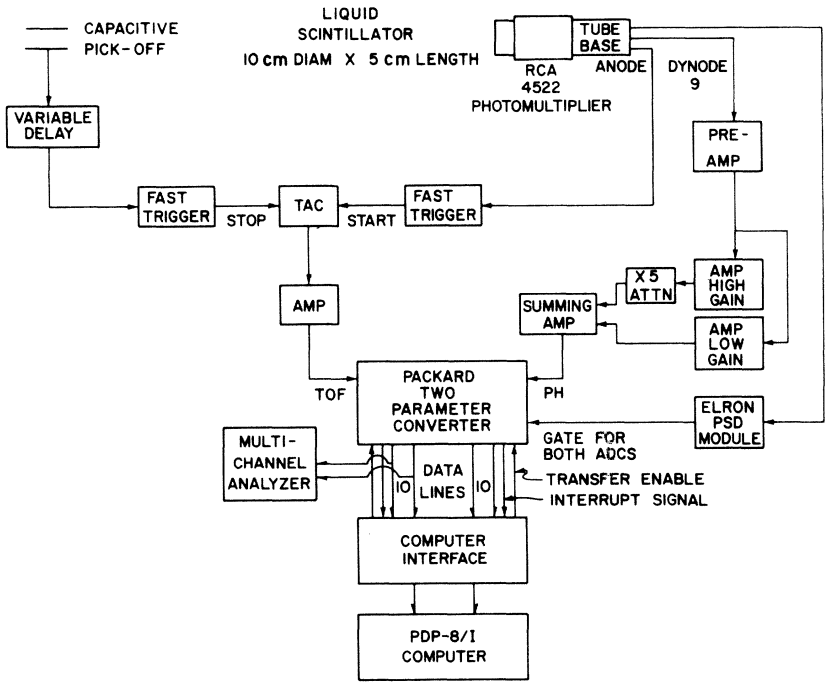

FIG. 2. Block diagram of electronics used in the dynamically biased time-of-flight system.

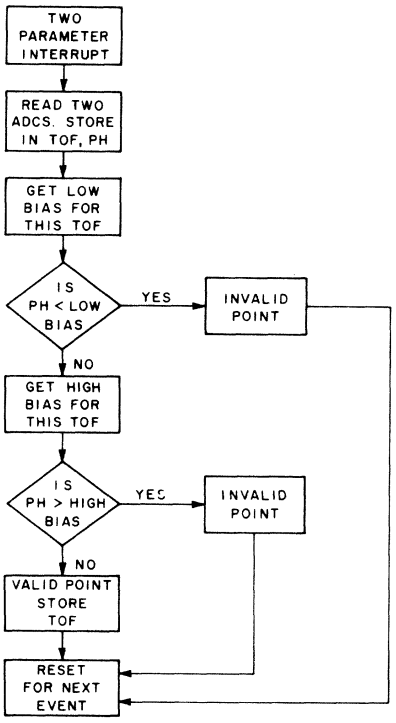

FIG. 3. Logic flow diagram of the computer program used to achieve dynamic biasing.

I are the characteristics of the polyethylene sample which was used for the absolute normalizations of the differential cross sections to the accurately known n-p scattering cross sections.

The Zr isotopes and the Mo isotopes were placed 6.3 cm and 8.2 cm, respectively, from the center of the neutron source. They were at 0° to the incident beam direction. The angular distributions were taken in ~10° increments from 30° to 156° (Zr) or 159° (Mo). Flight paths were 3.05 and 3.92 m for Mo and Zr, respectively. The yields for each angle were normalized to each other by means of the monitor detector. Typical measurements required 0.3 to 1.0 h for each sample at each angle, to obtain 1.0 to 3.0% statistical uncertainty in the subtracted yields of the elastic peaks in the time spectra.

The background contributions to the TOF spectra were determined by making measurements with the sample removed. The sample-out background was subtracted from the sample-in spectra point by point. Figure 4 shows TOF spectra for several of the isotopes at various angles. The time calibration of these TOF spectra is 0.46 nsec per channel. The TOF spectra also show a number of neutron groups from inelastic scattering. The determination of the absolute differential cross sections was made by comparison of a relative cross section at 40° to the well-known neutron-proton scattering cross section.[21] The number of neutrons scattered by hydrogen was determined by observing the TOF spectrum of neutrons scattered by polyethylene. Since the differential cross section of hydrogen for neutron scattering is isotropic in the center of mass system for 1.5-MeV neutrons, the laboratory differential cross section for angles less than 90° is

$$\sigma(\theta_{\text{lab}}) = \frac{\sigma_T \cos\theta_{\text{lab}}}{\pi} ,$$

where θ_{lab} is the neutron laboratory scattering angle and σ_T is the total n-p cross section.

Since the energy of a scattered neutron depends on the scattering angle and mass of the target, the efficiency of the neutron detector as a function of energy was needed. Because of the additional uncertainties introduced in an absolute efficiency measurement due to fluctuations and uncertainties in Li target thicknesses, only a relative detector

TABLE I. Description of scattering samples.

Sample	Isotopic composition (%)							Mass (g)	Diameter (cm)	Length (cm)
	^{92}Mo	^{94}Mo	^{95}Mo	^{96}Mo	^{97}Mo	^{98}Mo	^{100}Mo			
^{92}Mo	97.37	0.68	0.52	0.37	0.18	0.40	0.50	57.709	2.007	2.096
^{94}Mo	0.71	92.03	5.18	0.83	0.40	0.67	0.19	62.399	1.996	2.249
^{96}Mo	0.22	0.27	1.05	96.44	1.02	0.86	0.14	59.637	2.018	2.252
^{100}Mo	0.60	0.23	0.40	0.81	0.36	1.69	95.91	65.645	2.119	2.274
	^{90}Zr	^{91}Zr	^{92}Zr	^{94}Zr	^{96}Zr					
^{90}Zr	97.72	1.07	0.51	0.56	0.15			37.681	1.966	1.946
^{92}Zr	2.54	1.04	95.13	1.11	0.18			41.083	2.004	2.002
^{94}Zr	2.03	0.65	0.94	96.10	0.28			9.961	0.987	1.977
Polyethylene $(CH_2)_n$								0.708	0.1016 (i.d.) 0.6330 (o.d.)	2.525

efficiency was measured. The relative efficiency was determined using yields from the ^{7}Li(p,n)^{7}Be reaction and its absolute production cross sections. These cross sections have been determined by Gabbard and McPherson[22] at this laboratory for proton energies of 2.00 to 6.22 MeV and by Elbakr *et al.*[23] at the University of Alberta. The uncertainties in the absolute normalization of our measured differential cross sections have largely been determined by the accuracy of these measured ^{7}Li(p,n)^{7}Be cross sections. A measured efficiency curve is shown in Fig. 5 for the Zr experiment.

The elastic differential cross sections were corrected for the following: (a) deadtime in the counting electronics; (b) attenuation of the neutron flux in the samples; (c) angular resolution; and (d) multiple scattering of neutrons in the scattering samples. The deadtime in the counting electronics was typically 3 to 4%. The sample-in and sample-out TOF spectra were separately corrected for deadtime before subtraction.

The correction for attenuation of the incident and out-going neutron flux is based upon the method of Cranberg and Levin.[24] The corrections were 20 to 32% for all the scattering samples except ^{94}Zr. For the smaller ^{94}Zr sample the correction was 12%.

The angular spread at the detector was due primarily to the finite size of the scattering samples. The face of the neutron detector was 392.0 cm from the center of the sample and subtended an angle of less than 1.0°, and hence was not included in the angular resolution correction.

Multiple scattering calculations correct for neutrons that are scattered more than once in the scattering sample. The corrections for multiple-elastic scattering use the methods of Blok and Jonker[25] and Walt and Barschall.[26] Both the angular resolution and the multiple scattering corrections were made using a computer code written by Reber.[27] The multiple scattering corrections were also calculated using a computer code written by one of the authors (FDM) based upon the methods of Cox[28] and Kinney.[29] The different correction methods were found to agree to within 2.0%.

Because of the large neutron energy losses in scattering from hydrogen and carbon in the polyethylene sample, a Monte Carlo code was used to correct for outgoing flux attenuation and multiple scattering in polyethylene. The code was written by Smith[30] at Argonne National Laboratory and incorporates libraries of the total and differential cross sections for hydrogen and carbon. The incident flux attenuation correction for the poly-

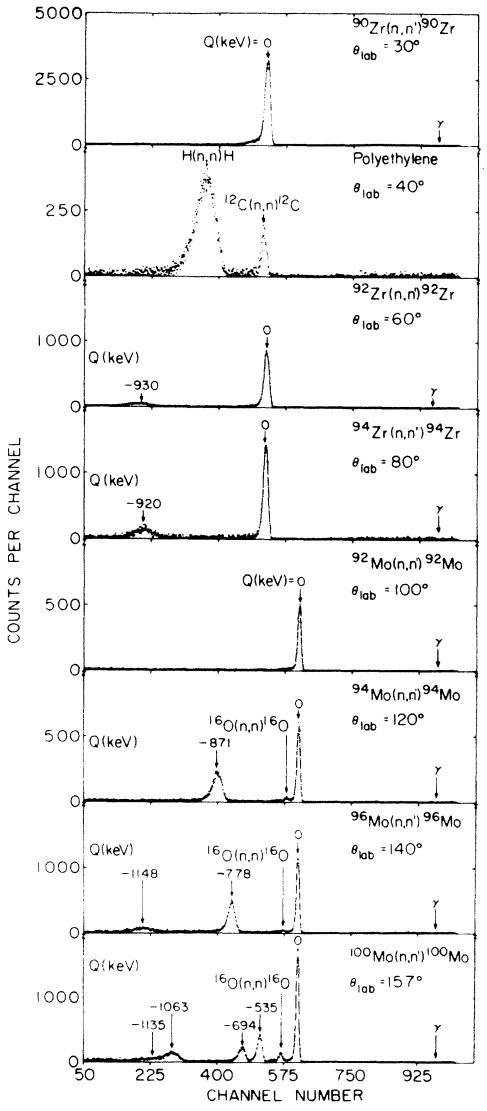

FIG. 4. Time-of-flight spectra for several of the isotopes at various neutron scattering angles. Sample-out background has been subtracted.

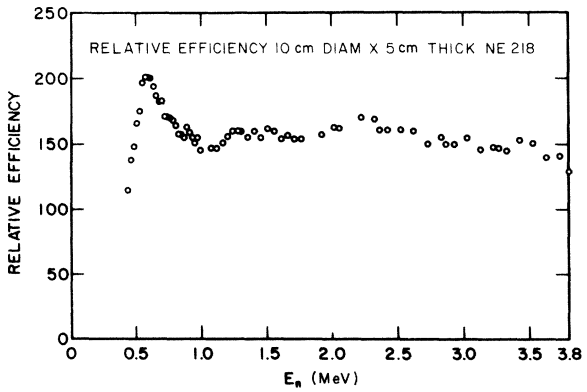

FIG. 5. The measured relative efficiency of the neutron detector as a function of neutron energy.

ethylene sample was based upon the method of Cranberg and Levin.[24] The resulting total attenuation and multiple scattering correction for the polyethylene sample was 16%.

In addition to the above corrections, a small correction was made to the measured elastic yields for the ^{100}Mo isotope. All of the Mo samples were found to have a small contamination due to oxygen in the samples. The effect was largest for the ^{100}Mo sample and much smaller for the remaining samples. The $^{16}O(n,n)^{16}O$ scattering peaks in the TOF spectra resulting from neutron scattering from ^{16}O nuclei are shown in Fig. 4. From the yields in these $^{16}O(n,n)^{16}O$ peaks a correction was derived and applied to the $^{100}Mo(n,n)^{100}Mo$ yields at the forward angles where the two peaks could not be resolved. For angles greater than 80° the peaks could be resolved and the $^{16}O(n,n)^{16}O$ yield was not included in the analysis. For the forward angles the correction amounted to 0.7% at 30° and 1.0% at 70°. Oxygen contamination to the other Mo isotopes was less than the amount present in the ^{100}Mo sample and no correction was made for it.

The inelastic differential cross sections were corrected for the following: (a) deadtime in the counting electronics; (b) attenuation of the neutron

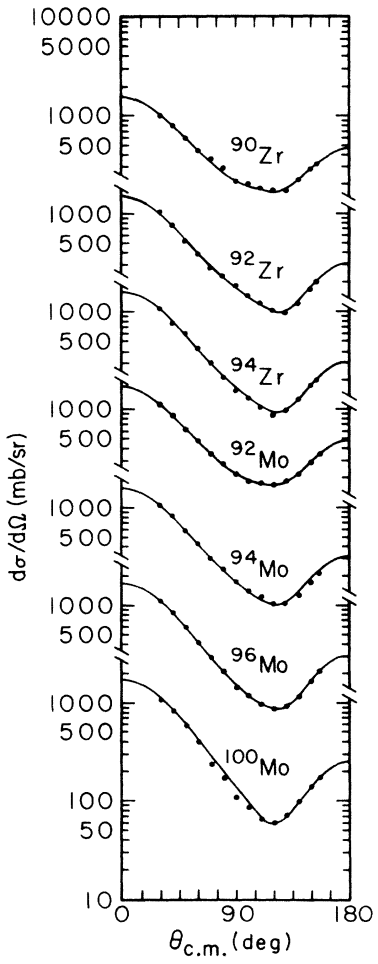

FIG. 6. Measured differential elastic cross sections for 1.5-MeV neutrons scattered by the isotopically enriched samples. The relative uncertainties are smaller than the actual data points. The normalization uncertainties which are listed in Table III, are less than 7.0% and are not shown on the figure. The solid lines are theoretical calculations discussed in Sec. V.

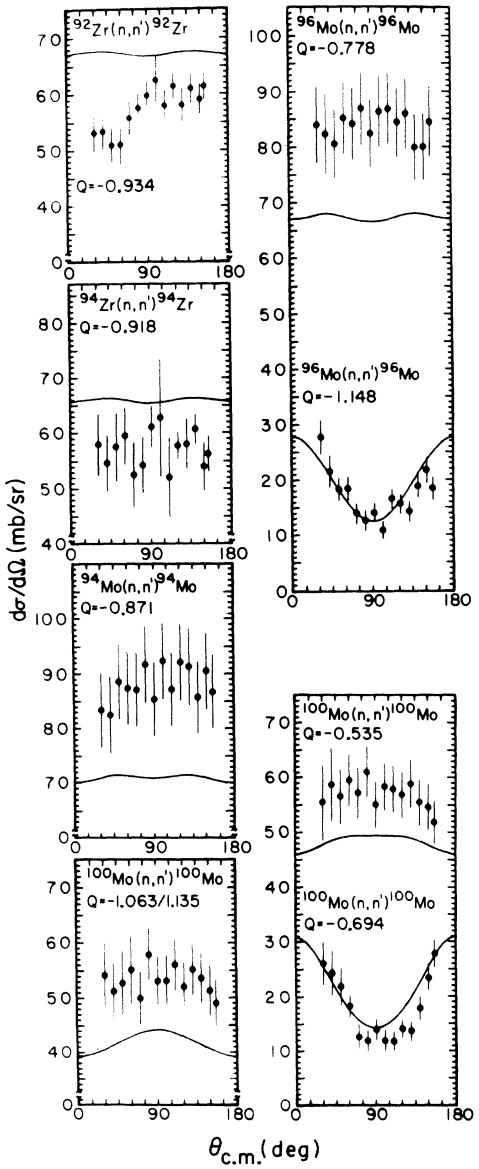

FIG. 7. The measured differential inelastic cross sections for 1.5-MeV neutrons scattered by the isotopically enriched samples. The error bars shown with each data point are relative uncertainties. The solid lines are theoretical calculations discussed in Sec. V. Some scales have suppressed zeros.

TABLE II. Legendre polynomial coefficients for fits to experimental elastic differential cross sections at 1.5 MeV. Coefficients have units of mb/sr.

	^{92}Mo		^{94}Mo		^{96}Mo		^{100}Mo		^{90}Zr		^{92}Zr		^{94}Zr	
L	Coeff.	Unc.	Coeff.	Unc.	Coeff.	Unc.	Coeff.	Unc.	Coeff.	Unc.	Coeff.	Unc.	Coeff.	Unc.
0	411.0	1.6	355.8	2.0	348.4	2.3	319.5	2.7	396.2	5.8	338.5	2.9	339.8	4.0
1	431.4	3.6	468.4	4.7	490.8	5.6	490.5	6.5	384.6	13.0	439.6	7.1	455.2	9.5
2	479.0	5.7	439.7	7.2	485.0	8.3	481.9	8.7	399.9	18.2	427.5	11.0	429.9	12.4
3	156.5	6.4	168.2	7.9	186.4	9.2	174.3	8.4	102.3	18.2	189.5	12.0	139.9	11.3
4	156.8	7.7	143.3	8.9	150.5	10.1	101.9	6.2	113.7	17.3	180.5	13.7	103.7	9.2
5	26.2	6.6	25.6	7.6	25.5	8.2					34.4	11.0		
6	39.0	6.2	25.4	6.8	31.2	6.6					26.3	9.3		

flux in the samples; and (c) multiple scattering of neutrons in the scattering samples.

The deadtime in the counting electronics and the flux attenuation corrections were determined in the same manner as for the elastic scattering. The inelastic multiple scattering corrections were calculated using a computer code written by one of the authors (FDM) based upon the methods of Engelbrecht.[31] The flux attenuation reduced the neutron flux in the samples while the inelastic multiple scattering had the effect of increasing the flux in the samples. The partially compensating effects of attenuation and inelastic multiple scattering resulted in correction of 20 to 25%, and 10 to 15%, respectively.

IV. EXPERIMENTAL RESULTS

A. Measured cross sections

The elastic differential cross section measurements are shown graphically in Fig. 6. The relative uncertainties are smaller than the size of the data points. The curves shown in the figure are theoretical cross section calculations which are discussed in Sec. V. The Legendre polynomial coefficients and their uncertainties, which describe the measured cross sections, are given in Table II. The least-squares fitting procedure of Cziffra and Moravcsik was used to determine these coefficients and their uncertainties.[32] The criteria used to determine the highest order polynomial included in the fit is discussed elsewhere.[27,33]

The inelastic cross section measurements are shown in Fig. 7. The error bars shown for each data point represent relative uncertainties only. The curves shown in the figure are theoretical cross section calculations which are discussed in Sec. V.

Contributing factors to the uncertainties in the measured cross sections were counting statistics, uncertainties from the previously mentioned corrections for finite sample size, the uncertainty in the detector efficiency as a function of neutron energy, and uncertainty in the neutron monitor. The uncertainty arising from the electronic deadtime corrections and the uncertainty in the n-p cross section are small. The sources of uncertainties and their magnitudes are given in Table III. The relative uncertainties are those contributing to the uncertainty in the shape of the angular distribution, and normalization uncertainties are those arising in the normalization of the angular distribution to the n-p cross section at the laboratory scattering angle of 40°.

B. Comparison with other measurements

Lambropoulos *et al.*[13] have made an extensive set of measurements of the differential elastic and inelastic cross sections and the total cross sections of ^{92}Mo, ^{94}Mo, ^{96}Mo, ^{98}Mo, and ^{100}Mo in the neutron energy range from 0.3 to 1.5 MeV. Their differential cross section measurements are made at energies typically separated by 20 keV with incident neutron energy spreads of ~20

TABLE III. Sources of uncertainty in the measured cross sections.

Source	Range	
Relative uncertainties		
	Elastic	Inelastic
Counting statistics	0.5–2.0%	6.0–13.0%
Monitor	<1.0%	<1.0%
Efficiency curve	<1.0%	<1.0%
Angular resolution correction	<1.0%	···
Multiple scattering corrections	<2.0%	···
Normalization uncertainties		
Flux attenuation and multiple scattering corrections	<1.5%	<3.0%
n-p cross section uncertainty	<1.0%	<1.0%
Efficiency curve	5.2%	5.2%[a]
n-p counting statistics	3.4%	3.4%
Total uncertainty	7.0–7.5%	9.0–15.0%

[a] Typical value.

keV. Thus their eight angle differential cross sections are not strictly comparable to our measurements at 1.50 MeV, with a neutron energy spread of ~80 keV. In order to compare the Kentucky data with the Argonne data, we have averaged, for each isotope, the Argonne data taken between 1.44 and 1.50 MeV. This will give an energy averaging interval comparable to the Kentucky data, but with an average energy 20 to 30 keV lower. The averaged Argonne data are shown in Fig. 8. Polynomial fits to these averaged results are shown by the dashed line. The polynomial fits to the data of the present experiment are shown by the solid curves in the same figure. These latter polynomial coefficients are given in Table II. At 40°, the angle of our normalization to the n-p cross section, the Argonne and Kentucky results differ by 2 to 8% with an average difference of 5%. This is well within the rms value of the claimed uncertainties of 5 to 10% and 7% for Argonne and Kentucky, respectively. It is seen from the curves in Fig. 8 that the difference between the two results in the region of the cross section minima is much greater than can be explained by the claimed experimental uncertainties.

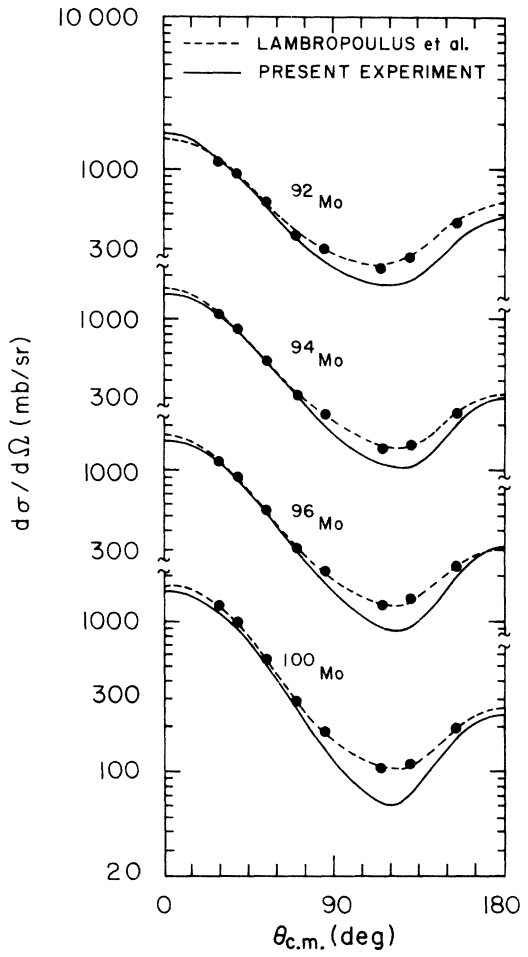

FIG. 8. Comparison of the Legendre polynomial fits to the measured molybdenum differential elastic cross sections for the present experiment with the results of Lambropoulos *et al.* (Ref. 13). The data points are the results of Ref. 13 averaged between 1.44 and 1.50 MeV.

One important difference between the Kentucky and Argonne measurements is that, whereas the Kentucky data is normalized to the known n-p cross section at 40°, the Argonne measurements are normalized to the previously measured[34] elastic differential cross sections of C. The polyethylene scatterer used here to observe the n-p scattering also gives a carbon elastic scattering peak in the time spectra, as seen in Fig. 4. The Kentucky data can also be compared to the carbon elastic differential cross section at 40°. Normalization of the Kentucky data at 40° to the carbon cross section[34] used by Lambropoulos *et al.*[13] would raise our cross sections by 13.4%. However, if the most recent carbon cross sections measured by Lane *et al.*[35] are used, the normalization of the Kentucky data to the carbon cross section would raise our cross sections 6.8%.

It should be noted that the two measurements[34,35] of the carbon differential cross section at this energy and angle differ by less than 7.0%, which is within the indicated uncertainties.[34,35] To clarify the normalization to carbon, we have remeasured the carbon differential cross section at 1.5 MeV. At $\theta_{lab} = 40°$ our measured carbon cross section is 1.2% lower than that given in Ref. 35, which gives a cross section for the Mo and Zr isotopes 5.6% larger than our n-p normalization.

The inelastic cross sections as well as the measured total cross sections of Lambropoulos *et al.*[13] may also be compared to the present results. This comparison is shown in Table IV. In this table the integrated elastic and inelastic cross sections are obtained from the polynomial fits to our data. A comparison of the inferred elastic cross sections shows that the integrated elastic results of Lambropoulos *et al.*[13] are larger than the present results by 300 to 600 mb for each isotope, or about 6 to 12%. The inelastic results for both measurements are in very good agreement for all excited levels except for the 694 keV level in ^{100}Mo. For this level the integrated cross section result of Lambropoulos *et al.*[13] is greater than the present result by almost a factor of 2.

By adding the appropriate integrated elastic and inelastic cross sections, the inferred total cross sections are obtained. The present inferred cross sections are compared to both the inferred total cross sections and measured total cross sections of Lambropoulos *et al.*,[13] averaged over the 1.44

to 1.50 MeV energy interval. The differences between our inferred total cross sections and the Argonne measured total cross sections range from 0.6% for ^{92}Mo to 7.3% for ^{96}Mo, with an average difference of 4.0%. This is well within our claimed normalization uncertainty of 7.0%.

C. Comparison of experimental results for different isotopes

A primary reason for making measurements on both the even-A isotopes of Mo and Zr is that a direct comparison can be made between two sets of isotopes which differ only by two protons; i.e., ^{90}Zr and ^{92}Mo, etc. The results of this comparison show that the addition of two protons makes only a small difference in the angular distribution of the elastic cross sections at this energy. The comparisons between the Legendre polynomial fits to the differential cross sections of ^{90}Zr and ^{92}Mo, ^{92}Zr and ^{94}Mo, and ^{94}Zr and ^{96}Mo are shown in the top panel of Fig. 9. The addition of neutrons, however, makes a larger difference in the angular distributions. The Legendre polynomial fits to the elastic differential cross sections of the Zr and Mo isotopes are shown in the middle and lower panels of Fig. 9. The minimum of the distribution is reduced with increasing neutron number at this energy.

The reason that the addition of two protons makes a smaller difference in the shape of the differential elastic cross section than the addition of two neutrons may be related to the almost degenerate nature of the proton shells involved ($2p_{1/2}$ and $1g_{9/2}$) and the large energy gap between the neutron shells ($1g_{9/2}$ and $2d_{5/2}$). For example, the addition of two protons to ^{90}Zr does not add as many low-lying levels as does the addition of two neutrons to ^{90}Zr. As the nuclear level density is increased, more of the reaction cross section is used in inelastic processes and less for compound elastic (CE) scattering. Thus, the minimum in the angular distribution, which is predominantly CE scattering, is reduced.

V. THEORETICAL ANALYSIS

The theoretical analysis presented with this paper is only part of an extensive study of neutron elastic and inelastic scattering from nuclei in the mass region from $A = 90$ to $A = 100$. An attempt will be made to obtain a consistent set of potential parameters to describe this mass region for incident energies of 1.5 to 8.5 MeV. Commonly used optical model potentials will be employed and varied to obtain the best χ^2 fits to the elastic differential cross sections. The potential parameters determined from elastic scattering will then

TABLE IV. Cross section comparison.

Isotope	Q [a]	σ_{el} [b]	σ_{inel} [b]	σ_t [c]	σ_{el} [d]	σ_{inel} [e]	σ_t [f]	σ_t [g]	Percent [h] difference
^{92}Mo	0.0	5165 ± 362		5165 ± 362	5734 ± 459		5734 ± 459	5198	0.6
^{94}Mo	0.0	4471 ± 313		5588 ± 335	4740 ± 379		5774 ± 395	5635	0.8
	−0.871		1117 ± 119			1034 ± 111			
^{96}Mo	0.0	4378 ± 307		5644 ± 326	4640 ± 371		5893 ± 388	6091	7.3
	−0.778		1057 ± 105			988 ± 108			
	−1.148		209 ± 31			265 ± 32			
^{100}Mo	0.0	4015 ± 281		5610 ± 300	4670 ± 374		6552 ± 403	6035	7.0
	−0.535		714 ± 66			665 ± 103			
	−0.694		211 ± 33			408 ± 56			
	−1.063		} 670 ± 76			} 809 ± 93			
	−1.135								

[a] Q value of excited level in MeV.

[b] Present elastic and inelastic results in mb; uncertainties given include both relative and normalization uncertainties.

[c] Present inferred total cross sections; rms uncertainties determined from the uncertainties in the elastic and inelastic cross sections.

[d] Elastic cross sections of Lambropoulos *et al.* (Ref. 13); actual values were obtained from the National Neutron Cross Section Center, Brookhaven National Laboratory (NNCSC) and were energy averaged from 1.44 to 1.50 MeV; uncertainties given as ±8%.

[e] Inelastic cross sections of Lambropoulos *et al.* (Ref. 13), actual values were obtained from NNCSC and were energy averaged from 1.44 to 1.50 MeV; uncertainties are simple averages of the uncertainties in the individual measurements.

[f] Inferred total cross sections of Lambropoulos *et al.* (Ref. 13); rms uncertainties were determined from the uncertainties in the elastic and inelastic results.

[g] Measured total cross sections of Lambropoulos *et al.* (Ref. 13), actual values were obtained from NNCSC and were energy averaged from 1.44 to 1.50 MeV; uncertainties in individual measurements are approximately ±2%.

[h] Percent difference $[(\sigma_t^g - \sigma_t^c)/\sigma_t^g] \times 100$.

be used to calculate inelastic cross sections without further change of these parameters.

A. Elastic differential cross sections

The complex potential chosen for the calculation was

$$V(r) = -Vf(r) - iWg(r) - Uh(r)\vec{l}\cdot\vec{\sigma}\,.$$

The real potential had a Woods-Saxon form, the imaginary potential had a Woods-Saxon derivative form, and the spin-orbit potential was real with a Thomas form. Therefore,

$$f(r) = \{1 + \exp[(r - r_0 A^{1/3})/a]\}^{-1},$$

$$g(r) = 4b\left|\frac{d}{dr}\{1 + \exp[(r - r' A^{1/3})/b]\}^{-1}\right|,$$

$$h(r) = \left(\frac{\hbar}{m_\pi c}\right)^2 \frac{1}{r}\left|\frac{d}{dr}[f(r)]\right|.$$

At the incident energy of 1.5 MeV, compound nucleus contributions are expected to be large, especially at the minima of the angular distributions. The elastic scattering was assumed to be an incoherent sum of shape-elastic scattering and compound-elastic (CE) scattering. The shape-elastic scattering was calculated using an optical model code JIB [36] which contained a search routine. The contribution of CE scattering was determined using the computer code ALTE [37] which incorporates the Wolfenstein[38]–Hauser-Feshbach[39] (WHF) formalism and includes resonance-width-fluctuation corrections.[40,41]

It was evident during the fitting procedure that most of the cross section near the minimum in

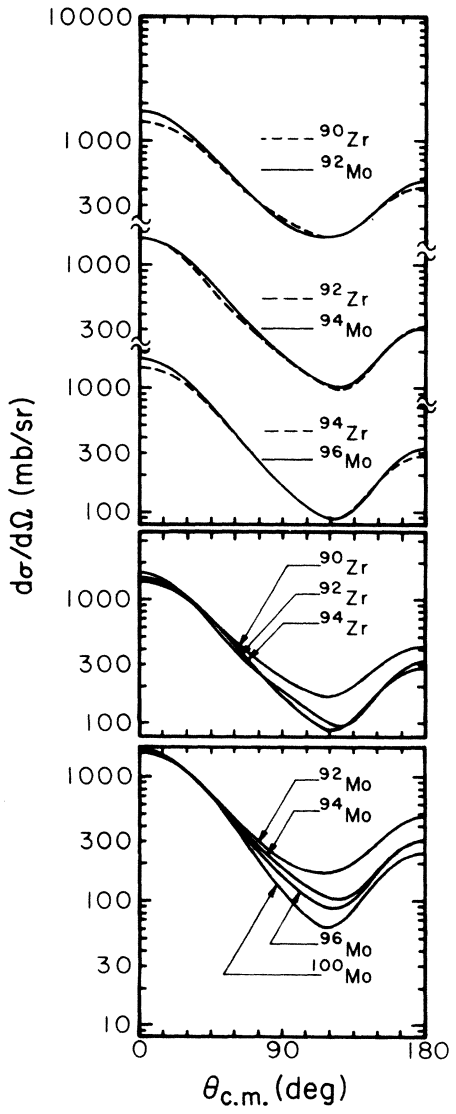

FIG 9. Comparisons between the Legendre polynomial fits to the measured differential elastic cross sections of the zirconium and molybdenum isotopes.

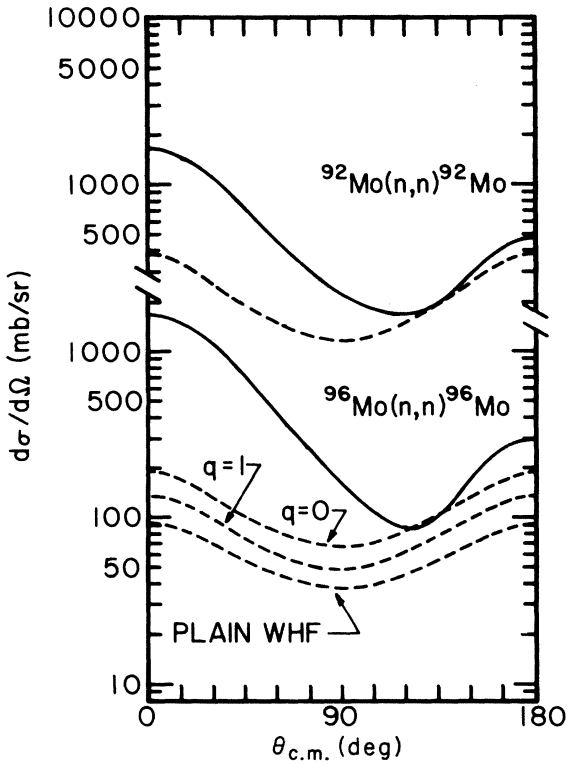

FIG. 10. The polynomial fits to the differential elastic cross sections for 1.5-MeV neutrons scattered by ^{92}Mo and ^{96}Mo are shown by the solid lines. The dashed lines represent calculated compound elastic cross sections as discussed in Sec. V. The final theoretical fits to the data are nearly identical to the polynomial fits shown.

each of the elastic differential cross sections was CE scattering. The method of calculating the CE cross sections, that is, how to include resonance-width-fluctuation effects which can alter the CE cross section by as much as a factor of 2 or 3, was crucial to the fitting procedure. However, optical model potentials could be determined independent of this question since in ^{90}Zr and ^{92}Mo, the incident neutron energy is below the threshold for inelastic scattering, and the CE cross section can be determined directly from the WHF formalism without modification. Further, the fact that the measured elastic cross section of ^{90}Zr proved to be nearly identical with that of ^{92}Mo, within uncertainties, suggests that it might be possible to fit the complete set of data with a single set of optical model parameters. This is shown in Fig. 9, where it is also clear that other pairs of nuclei with similar level structure also have nearly identical cross sections. Figure 10 shows the results of the fitting procedure for ^{92}Mo. At the minimum and at back angles, the CE cross section is dominant. Using the optical model potentials obtained from fitting ^{90}Zr and ^{92}Mo, fits to the other nuclei were attempted. The problem of how to handle the CE cross section in the fitting procedure is illustrated for ^{96}Mo in Fig. 10. In this illustration, the full width fluctuation correction of Dresner[40] and Lane and Lynn[41] ($q = 0.0$) provided too much CE cross section at the minimum in the differential cross section while the plain WHF calculation did not provide enough. In order to obtain good fits at the minima of the differential cross sections for all the nuclei it was necessary to employ the full width-fluctuation correction and, in addition, to modify the optical model transmission coefficients as suggested by Moldauer.[42] The conventional optical model transmission coefficients T were replaced by

$$T' = T + \frac{1}{q}\left[1 - (1 - qT)^{1/2}\right]^2 ,$$

where the parameter q is a measure of nuclear level overlap. It can vary between zero for isolated levels and one for strongly overlapping levels. The value of q was adjusted to best fit the elastic differential cross sections and was found to be $q = 0.5$.

In most cases the fits obtained were very good and are shown in Fig. 6. All curves were obtained using one set of optical model parameters obtained by fitting the neutron elastic scattering angular distribution of ^{90}Zr and ^{92}Mo. These parameters are given in Table V. Since the present experiment did not include any polarization measurements and hence did not offer any guidance for the selection of a spin-orbit strength, a typical value of 5.5 MeV was used. The value of the s-wave strength function determined from these optical model parameters was 0.5×10^{-4} and is in reasonable agreement with experimental values in this mass region.

TABLE V. Optical model parameters used to fit the elastic differential cross sections of the Mo and Zr isotopes for 1.5 MeV neutrons. Potential strengths are in MeV and radii and diffusenesses are in fm.

$V = 48.3$	$W = 6.7$	$U = 5.5$	
$r_0 = 1.25$	$r' = 1.30$	$r_0 = 1.25$	$q = 0.5$
$a = 0.65$	$b = 0.47$	$a = 0.65$	

During the fitting procedure, a small dependence of the real central strength V upon neutron excess $(N - Z)/A$ was found. The effect was masked by the relatively large CE contributions at this energy. A much stronger evidence for a dependence upon neutron excess has been found at higher energies where compound nucleus contributions to the elastic scattering are not as large.[43] Hence, for the present work a single set of optical model parameters was sufficient to fit the data.

B. Inelastic differential cross sections

Theoretical fits obtained to the inelastic differential cross sections were calculated from the WHF formalism with level-width-fluctuation corrections of Dresner[40] and Lane and Lynn[41] and with transmission coefficients modified according to Moldauer.[42] All calculations were made using the same set of parameters and a value of $q = 0.5$ which were found to give such good agreement between experiment and theory for the elastic scattering. The calculated fits are shown as solid lines in Fig. 7. The fits are reasonably good and agree to within 20% with the measured inelastic differential cross sections. The first excited states in ^{90}Zr and ^{92}Mo were not excited at this energy. The excited $J^\pi = 0^+$ states in ^{96}Mo at 1.148 MeV and ^{100}Mo at 0.694 MeV are exceptionally well fitted. The calculations for the other excited states in ^{94}Mo, ^{96}Mo, and ^{100}Mo are lower than the experimental cross sections by approximately 12 to 20%.

The normalizations of the inelastic differential cross sections for the first excited states in ^{92}Zr at 0.934 MeV and ^{94}Zr at 0.918 MeV are uncertain because the energies of these scattered neutrons were on a very rapidly changing portion of the efficiency curve. For the Zr cross section measurements, the detector bias level was substantially higher than for the Mo measurements. Hence, the detector efficiency curve for the Zr experiment did not extend as low in energy as for the Mo experiment. The efficiency curve used

for the measurements on the Zr isotopes only is shown in Fig. 5. Because of especially large uncertainties in the detector efficiency for these two groups of scattered neutrons ($Q = -0.934$ and $Q = -0.918$ MeV), the normalizations of the differential cross sections are uncertain by approximately 50%, and the theoretical fits have little significance.

VI. CONCLUSIONS

The experimental results presented here for the even-A isotopes of Mo and Zr were obtained with relative and over-all normalization uncertainties of 3.5 and 7.0%, respectively.

A comparison between the cross sections for the two sets of isotopes has shown the cross sections to be very similar. The addition of two protons has been shown to have only a small effect upon the differential cross sections. The addition of two neutrons has been shown to have a larger effect especially near the minima in the angular distributions. The minima decrease quite dramatically with increasing neutron number.

The present experimental results obtained for the Mo isotopes were compared to the results of Lambropoulos *et al.*,[13] with their results averaged over our energy spread. The agreement between the two sets of elastic differential cross sections are within normalization uncertainties except near the minima in the distributions. The integrated elastic cross sections of Lambropoulos *et al.*[13] are consistently larger than the present experimental results by about 6 to 12%. The total cross sections inferred from our measured elastic and inelastic cross sections are in quite good agreement with the directly measured *total* cross sections of Lambropoulos *et al.*[13] The inelastic cross sections to all levels, measured at the two laboratories, were found to be in excellent agreement except for the 0.694 MeV level in ^{100}Mo, where the results of Lambropoulos *et al.*[13] are larger than the present results by almost a factor of 2. It should be noted that the theoretical fit obtained here for the 0.694 MeV level is in excellent agreement with our present results, and is one of our best fits.

During the analysis it was observed that the majority of the differential elastic cross section at the minimum was due to compound nucleus contributions. In addition, the value of the CE cross section which gave the best fit to the elastic differential cross section was in all cases less than the cross section given by the full $q = 0.0$ resonance-width-fluctuation correction of Dresner[40] and Lane and Lynn.[41] The best fits were obtained by employing both the full resonance-width-fluctuation correction and the Moldauer[42] modification of the optical model transmission coefficients with a value of $q = 0.5$.

A small neutron excess dependence in the real central strength was found during the fitting procedure which, because of the large contribution of CE scattering, could not be determined with any accuracy. Hence, a single set of optical model parameters was sufficient to describe the entire set of data. The calculated results for elastic scattering were very good. The worst fit was obtained to the differential cross section of ^{100}Mo where one would expect to observe the largest dependence upon neutron excess. The calculated fits obtained to the inelastic differential cross sections were 10 to 20% lower than the measured values except for the $J^{\pi} = 0^+$ excited states, which were fitted exceptionally well.

ACKNOWLEDGMENTS

The authors would like to thank Professor M. T. McEllistrem and Mr. David Waterfill for assistance in taking data and for many helpful discussions. We would also like to thank the University of Kentucky Computing Center for supplying time necessary for the analysis of data.

---

*Work supported in part by the National Science Foundation.

†Present address: Department of Physics, North Texas State University, Denton, Texas 76203.

‡Mailing address: 4827 Isabella Avenue, Montreal, Quebec, Canada.

[1]K. C. Chung, K. Swartz, A. Mittler, C. Robertson, J. D. Brandenberger, and M. T. McEllistrem, Bull. Am. Phys. Soc. 14, 1238 (1969).

[2]K. C. Chung, K. Swartz, J. D. Brandenberger, and M. T. McEllistrem, Bull. Am. Phys. Soc. 15, 499 (1970).

[3]M. T. McEllistrem, G. P. Glasgow, K. Sinram, and J. D. Brandenberger, Bull. Am. Phys. Soc. 16, 619 (1971).

[4]C. E. Robertson, K. C. Chung, K. Sinram, J. D. Brandenberger, and M. T. McEllistrem, Bull. Am. Phys. Soc. 16, 620 (1971).

[5]K. Sinram, K. C. Chung, C. E. Robertson, J. D. Brandenberger, and M. T. McEllistrem, Bull. Am. Phys. Soc. 16, 620 (1971).

[6]M. T. McEllistrem, K. Sinram, C. E. Robertson, and J. D. Brandenberger, Bull. Am. Phys. Soc. 16, 1154 (1971).

[7]K. C. Chung, J. D. Brandenberger, M. T. McEllistrem, and T. B. Grandy, Bull. Am. Phys. Soc. 15, 1693

(1970); K. Sinram, K. C. Chung, J. D. Brandenberger, and M. T. McEllistrem, Bull. Am. Phys. Soc. 15, 1692 (1970).
[8]J. D. Brandenberger, K. C. Chung, K. Sinram, G. P. Glasgow, C. E. Robertson, and M. T. McEllistrem, Bull. Am. Phys. Soc. 16, 1181 (1971).
[9]G. P. Glasgow, K. Sinram, J. D. Brandenberger, and M. T. McEllistrem, Bull. Am. Phys. Soc. 17, 901 (1972).
[10]K. Sinram, J. D. Brandenberger, and M. T. McEllistrem, Bull. Am. Phys. Soc. 17, 901 (1972).
[11]F. D. McDaniel, J. D. Brandenberger, M. T. McEllistrem, and G. P. Glasgow, Bull. Am. Phys. Soc. 18, 260 (1973).
[12]M. T. McEllistrem, J. D. Brandenberger, K. Sinram, G. P. Glasgow, and K. C. Chung, Phys. Rev. C 9, 670 (1974).
[13]P. Lambropoulos, P. Guenther, A. Smith, and J. Whalen, Nucl. Phys. A201, 1 (1973); P. A. Moldauer and A. B. Smith, in *Proceedings of the Third Conference on Neutron Cross Sections and Technology, Knoxville, Tennessee, 1971,* edited by J. A. Harvey and R. L. Macklin (U. S. Atomic Energy Commission), Vol. 1, Conf.-710301, p. 154.
[14]A. B. Smith and R. Hayes, Nucl. Phys. A93, 609 (1967).
[15]L. Cranberg, T. A. Oliphant, J. S. Levin, and C. D. Zafiratos, Phys. Rev. 159, 969 (1967).
[16]L. Cranberg, in *Progress in Fast Neutron Physics,* edited by G. C. Phillips, J. B. Marion, and J. R. Risser (Univ. of Chicago Press, Chicago, 1963), p. 89.
[17]J. D. Brandenberger and T. B. Grandy, Nucl. Instrum. Methods 93, 495 (1971).
[18]R. C. Mobley, Phys. Rev. 88, 360 (1952).
[19]R. C. Mobley and B. R. Albritton, Phys. Rev. 98, 232 (1955).
[20]L. Cranberg, R. A. Fernald, F. S. Hahn, and E. F. Shrader, Nucl. Instrum. Methods 12, 335 (1961).
[21]J. L. Gammel, in *Fast Neutron Physics,* edited by J. B. Marion and J. L. Fowler (Interscience, New York, 1963), Part II, p. 2209.
[22]F. Gabbard and M. R. McPherson, private communication.
[23]S. A. Elbakr, I. J. Van Heerden, W. J. McDonald, and G. C. Neilson, Nucl. Instrum. Methods 105, 519 (1972).
[24]L. Cranberg and J. S. Levin, Los Alamos Scientific Laboratory Report No. LA-2177 (1959).
[25]J. Blok and C. C. Jonker, Physica (Utr.) 18, 809 (1952).
[26]M. Walt and H. H. Barschall, Phys. Rev. 93, 1062 (1954); and M. Walt, Ph.D. thesis, University of Wisconsin, 1953 (unpublished).
[27]J. D. Reber, Ph.D. thesis, University of Kentucky, 1967 (unpublished).
[28]S. A. Cox, Nucl. Instrum. Methods 56, 245 (1967).
[29]W. E. Kinney, Nucl. Instrum. Methods 83, 15 (1970).
[30]A. B. Smith, Argonne National Laboratory, Argonne, Illinois 60439, private communication.
[31]C. A. Engelbrecht, Nucl. Instrum. Methods 80, 187 (1970); 93, 103 (1971).
[32]P. Cziffra and M. J. Moravcsik, University of California Radiation Laboratory Report No. UCRL-8523, 1959 (unpublished).
[33]J. D. Brandenberger, A. Mittler, and M. T. McEllistrem, Nucl. Phys. A196, 65 (1972).
[34]R. O. Lane, A. S. Langsdorf, Jr., J. E. Monahan, and A. J. Elwyn, Ann. Phys. (N. Y.) 12, 135 (1961); A. S. Langsdorf, Jr., R. O. Lane, and J. E. Monahan, Argonne National Laboratory Report No. ANL-5567-(Rev.), 1961 (unpublished); R. O. Lane, A. S. Langsdorf, Jr., J. E. Monahan, and A. J. Elwyn, Report No. ANL-6172, 1960 (unpublished).
[35]R. O. Lane, R. D. Koshel, and J. E. Monahan, Phys. Rev. 188, 1618 (1969); R. O. Lane, private communication.
[36]F. G. Perey, Phys. Rev. 131, 745 (1963).
[37]W. R. Smith, Comput. Phys. Commun. 1, 106, 181 (1969); Oak Ridge National Laboratory Report No. ORNL-TM-1117, 1965 (unpublished).
[38]L. Wolfenstein, Phys. Rev. 82, 690 (1951).
[39]W. Hauser and H. Feshbach, Phys. Rev. 87, 366 (1952).
[40]L. Dresner, Oak Ridge National Laboratory Report No. ORNL-CF-57-6-2, 1957 (unpublished).
[41]A. M. Lane and J. E. Lynn, Proc. Phys. Soc. Lond. 70, 557 (1957).
[42]P. A. Moldauer, Rev. Mod. Phys. 36, 1079 (1964).
[43]F. D. McDaniel, J. D. Brandenberger, M. T. McEllistrem, K. Sinram, and G. P. Glasgow, Bull. Am. Phys. Soc. 18, 1402 (1973).